

JGR Biogeosciences



METHOD

10.1029/2023JG007550

Key Points:

- Marsh Ecosystem Response to Increased Temperatures (MERIT) is a novel ecosystem warming experiment in a high-energy coastal salt marsh
- MERIT achieves passive aboveground and active belowground warming to 1 m soil depth
- MERIT tests warming effects on ecosystem functioning along a marine-terrestrial ecotone

Supporting Information:

Supporting Information may be found in the online version of this article.

Correspondence to:

R. L. Rich,
richr@si.edu

Citation:

Rich, R. L., Mueller, P., Fuß, M., Gonçalves, S., Ostertag, E., Reents, S., et al. (2023). Design and assessment of a novel approach for ecosystem warming experiments in high-energy tidal wetlands. *Journal of Geophysical Research: Biogeosciences*, 128, e2023JG007550. <https://doi.org/10.1029/2023JG007550>

Received 27 APR 2023

Accepted 22 SEP 2023

Author Contributions:

Conceptualization: Roy L. Rich, Peter Mueller, Lars Kutzbach, Kai Jensen, Stefanie Nolte

Data curation: Roy L. Rich, Allegra Tashjian, Simon Thomsen





Formal analysis: Roy L. Rich, Stefanie Nolte

Funding acquisition: Roy L. Rich, Peter Mueller, Lars Kutzbach, Kai Jensen, Stefanie Nolte

© 2023 Smithsonian Institution and The Authors.

This is an open access article under the terms of the [Creative Commons Attribution-NonCommercial-NoDerivs](https://creativecommons.org/licenses/by-nc-nd/4.0/) License, which permits use and distribution in any medium, provided the original work is properly cited, the use is non-commercial and no modifications or adaptations are made.

Design and Assessment of a Novel Approach for Ecosystem Warming Experiments in High-Energy Tidal Wetlands

Roy L. Rich^{1,2} , Peter Mueller^{1,2,3}, Miriam Fuß^{4,5} , Salomé Gonçalves¹, Eva Ostertag¹ , Svenja Reents¹ , Hao Tang^{1,6}, Allegra Tashjian², Simon Thomsen¹, Lars Kutzbach^{4,5}, Kai Jensen¹, and Stefanie Nolte^{7,8}

¹Institute of Plant Sciences and Microbiology, Universität Hamburg, Hamburg, Germany, ²Smithsonian Environmental Research Center, Edgewater, MD, USA, ³Institute of Landscape Ecology, Münster University, Münster, Germany, ⁴Institute of Soil Science, Department of Earth System Sciences, Universität Hamburg, Hamburg, Germany, ⁵Center for Earth System Research and Sustainability, Universität Hamburg, Hamburg, Germany, ⁶Key Laboratory of Land Resources Evaluation and Monitoring in Southwest, Ministry of Education, Sichuan Normal University, Chengdu, China, ⁷School of Environmental Sciences, University of East Anglia, Norwich Research Park, Norwich, UK, ⁸Centre for Environment, Fisheries and Aquaculture Science, Lowestoft, UK

Abstract Coastal salt marshes have an important role in climate change adaptation and mitigation. Direct and indirect responses to warming are expected to vary along the marsh elevation gradient, making ecosystem responses to warming at this marine-terrestrial ecotone uncertain. The Marsh Ecosystem Response to Increased Temperatures (MERIT) experiment was established in 2018 on the North Sea coast of Germany. Experimental plots are evenly distributed over three elevational marsh zones (pioneer, low marsh, and high marsh) and include three temperature treatments (ambient, +1.5°C, +3.0°C). MERIT's novel design combines active warming (horizontal surface warming cables and vertical soil warming pins) with passive, partially covered domes. For performance assessment, temperature deltas between ambient and warmed plots were calculated and evaluated at seasonal, daily, and diurnal timescales. We used Linear Mixed Models with Residual Maximum Likelihood for evaluating warming treatment effects and constraining environmental factors. MERIT was effective at ecosystem warming in this high-energy environment both above- and belowground. Mixed models show that warming treatment dominates temperature differences belowground and at the soil surface, along with factors such as wind speed, flooding duration, and solar radiation. Aboveground warming was lower than belowground warming, but the dome design minimized issues seen in other open-top chamber experiments. The combination of passive aboveground warming with feedback-controlled active surface and belowground heating provides a setup for understanding warming effects on tidal ecosystems without altering the natural impacts of wind, radiation, and tidal inundations at high-energy coastlines. Our design creates opportunities to expand future warming experiments to remote locations and technically challenging environments.

Plain Language Summary Coastal vegetated ecosystems such as salt marshes have been highlighted for their important role in climate change adaptation and mitigation, especially in storing carbon. However, responses of ecosystem functioning and biogeochemistry to warming are largely unknown and expected to differ based on hydrology. The Marsh Ecosystem Response to Increased Temperatures (MERIT) experiment was established in 2018 in a Wadden Sea salt marsh and spans the entire salt marsh elevation gradient with pioneer, low marsh, and high marsh vegetation communities. Our objective is to create a novel ecosystem warming design that can be used in coastal wetland ecosystems prone to tidal flooding and wave disturbance. The MERIT experiment is effective at warming this dynamic ecosystem. Mixed models show the warming treatment factor dominates temperature differences belowground and at the soil surface. Aboveground performance was lower than that of the belowground treatments but better than previous experiments. Performance increased with decreasing wind speed and increased solar radiation. Our study improves understanding between biological systems and global warming. This novel experiment allows us to directly quantify ecosystem response to warming, while allowing for tidal inundation to continue.

1. Introduction

Coastal vegetated ecosystems such as mangrove forests, seagrass beds, and tidal marshes have been highlighted for their important role in climate change adaptation and mitigation (Duarte et al., 2013). These ecosystems are

Investigation: Roy L. Rich, Miriam Fuß, Salomé Gonçalves, Eva Ostertag, Svenja Reents, Hao Tang, Simon Thomsen

Methodology: Roy L. Rich, Simon Thomsen

Project Administration: Simon Thomsen, Lars Kutzbach, Kai Jensen, Stefanie Nolte

Resources: Kai Jensen

Software: Roy L. Rich, Simon Thomsen

Supervision: Roy L. Rich, Simon Thomsen, Lars Kutzbach, Kai Jensen, Stefanie Nolte

Visualization: Roy L. Rich, Allegra Tashjian, Kai Jensen, Stefanie Nolte

Writing – original draft: Roy L. Rich, Peter Mueller, Miriam Fuß, Salomé Gonçalves, Eva Ostertag, Svenja Reents, Hao Tang, Kai Jensen, Stefanie Nolte

Writing – review & editing: Roy L. Rich, Peter Mueller, Allegra Tashjian, Lars Kutzbach, Kai Jensen, Stefanie Nolte

suggested as a nature-based solution for adaptation to sea level rise (SLR) and increased storminess (Duarte et al., 2013; Temmerman et al., 2013). Furthermore, they sequester disproportionately large amounts of “blue carbon” (McLeod et al., 2011), making conservation and restoration of these ecosystems promising measures for climate change mitigation. Because of their potential for climate change mitigation, understanding the possible effects of warming on these blue carbon ecosystems is vital. Experimental approaches to study effects of climate change on these tidal ecosystems are scarce and challenging to execute, largely because these ecosystems coincide with dynamic, high-energy environments that experience regular flooding and extreme storminess.

Tidal marshes form along coasts and estuaries, and global total area estimates vary from 2.2 to 40 Mha (Pendleton et al., 2012), including 5.5 Mha of salt marsh (Mcowen et al., 2017). Abiotic conditions can vary greatly within a single marsh site (Mueller et al., 2020), as salt marshes often span an elevational gradient from below mean high tide to above mean spring tide levels. Elevation is the primary factor controlling flooding frequency and vegetation spatial distribution. For example, in Wadden Sea marshes in Germany, vegetation usually forms three distinct zones (Figure 1). Flooding also drives sedimentation-associated surface-elevation change (i.e., minerogenic marsh formation, Nolte et al., 2013a) and is closely linked to vegetation succession (Nolte et al., 2019). Consequently, studies of salt marsh ecosystem function focus on elevation while salt marsh climate change studies concentrate on accelerated rates of SLR (Kirwan & Guntenspergen, 2012, 2015; Mueller et al., 2016; Reents et al., 2021). Here, we hypothesize shifts in the relative importance of hydrology and climatic conditions in driving processes along the elevation gradient. Hydrology—and the resulting low soil oxygen availability—drives processes at lower elevations (e.g., pioneer zone, Figure 1). Climate factors, like increased temperatures resulting from global warming, drive processes at higher elevations (e.g., high marsh [HM] zone, Figure 1). In the low marsh (LM), subsoils are generally waterlogged and anaerobic; the resulting low redox potential suppresses positive effects of higher temperatures on soil microbial carbon cycling. In contrast, in the HM (Figure 1) the upper soil is generally aerobic (Mueller et al., 2020), and belowground processes are more affected by climatic conditions, especially temperature. Warming studies in boreal peatlands show that warming effects on soil decomposition are less pronounced in more reduced waterlogged subsoils (lower elevations) compared to less reducing topsoils (higher elevations) (Hopple et al., 2020; Wilson et al., 2016). In the HM, warming would increase soil organic matter decomposition through increased microbial activity, leading to increased fluxes of greenhouse gases from the marsh to the atmosphere. Warming would increase plant productivity (see Charles and Dukes (2009) and Gedan and Bertness (2010)), especially in the HM (Figure 1).

In addition to these direct effects increasing decomposition and productivity, there may be indirect effects of warming, as increased productivity may enhance plant-mediated sediment deposition (Fagherazzi et al., 2012; Nolte et al., 2013a) (Figure 1). Through surface elevation change via sediment accretion, warming may indirectly change vegetation successional trajectories across the system (Nolte et al., 2013a).

To understand direct and indirect effects of warming on ecosystem functioning and succession in salt marshes, we established a novel in situ whole ecosystem warming experiment in a high-energy Wadden Sea salt marsh with a combination of active belowground and passive aboveground warming. Ecosystem manipulation experiments with feedback-controlled (or active) temperature control are extremely rare, exist mostly among terrestrial systems, and seldom have combined above- and belowground warming (Rich et al., 2015). Only two examples exist in wetland ecosystems (Hanson et al., 2017; Noyce et al., 2019), and these are both situated in organic soils and non-tidal or micro-tidal systems. Passive open-top chamber (OTC) experiments in the field have limited success in warming salt marsh ecosystems (Carey et al., 2018). Issues with OTC experiments include strong diurnal patterning with effective daytime warming and no warming or even temperature reduction at night (Carey et al., 2018; Gedan & Bertness, 2010), low effective warming during the summer as compared to other parts of the year, and only modest or no belowground warming (Zhong et al., 2013). Passive aboveground warming experiments are often chosen for remote locations but are disadvantageous because key ecosystem processes like decomposition occur belowground. Altogether, we consider these experiments to be insufficient to realistically analyze coastal ecosystems under global warming scenarios. Our aim is to achieve warming treatments which follow the seasonal, daily, and diurnal dynamics of temperatures at ambient conditions.

Marsh Ecosystem Response to Increased Temperatures (MERIT) was established in 2018 in a Wadden Sea salt marsh. It spans the entire salt marsh elevation gradient with pioneer (PIO), LM, and HM vegetation communities (Figure 1). In MERIT, we couple a passive aboveground dome approach with active surface and belowground soil warming to 1.0 m depth. Our design actively warms (Rich et al., 2015) using horizontal surface cables and

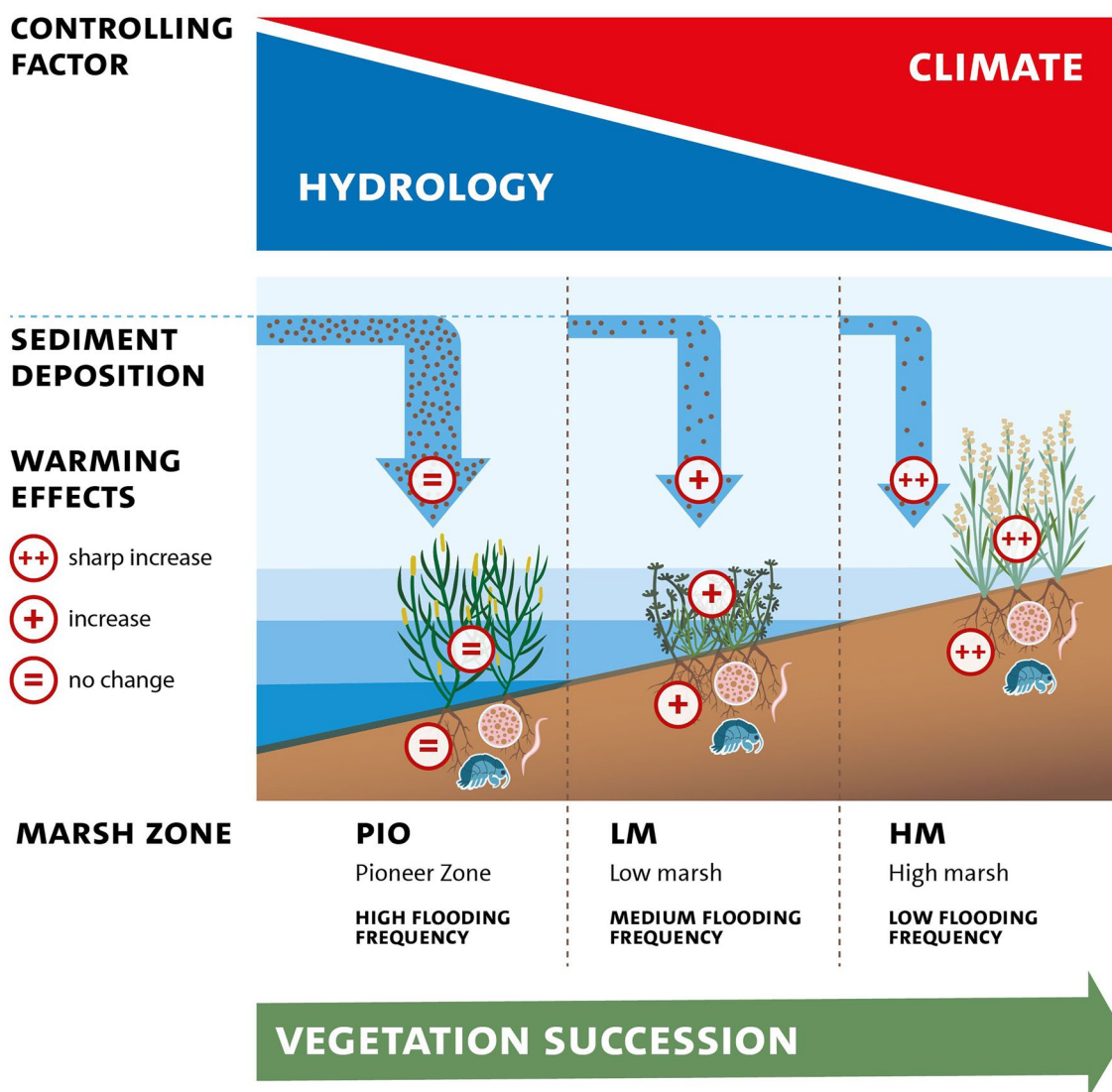


Figure 1. Conceptual figure illustrating the salt marsh zonation (pioneer, low marsh, high marsh) with flooding frequency, sedimentation, and vegetation succession. Hydrology is the controlling factor of processes in lower zones while climate becomes more relevant in higher zones. Warming in conjunction with hydrology will have strong positive effects (++), moderate positive effects (+), or no effects (=).

vertical resistance pins (Noyce et al., 2019; Reich et al., 2020). Integrated microprocessor-based feedback control creates a fixed temperature delta from ambient conditions for each marsh zone (ambient, +1.5°, or +3.0°C treatments). An in situ warming experiment with a similar design is currently deployed in a microtidal, low-energy, brackish estuarine wetland with organic soils in Maryland, USA (tidal amplitude of 0.4 m, Noyce et al., 2019). The Wadden Sea salt marshes experience stronger tidal fluctuations (tidal amplitude of approximately 3 m) and much higher wind speeds. The aim of this study is therefore to assess the above- and belowground performance of warming applied in the MERIT experiment under these challenging, dynamic environmental conditions.

2. Materials and Methods

2.1. Study Site

MERIT was established in the salt marsh of Hamburger Hallig (54°36′06.7″N 8°48′57.4″E) at the North Sea coast of Germany (Figures 2a and 2b). Hamburger Hallig was a small island until 1874, when it was connected to the mainland by a 3.5 km long dam, leading afterward to the expansion of salt marshes via so-called sedimentation

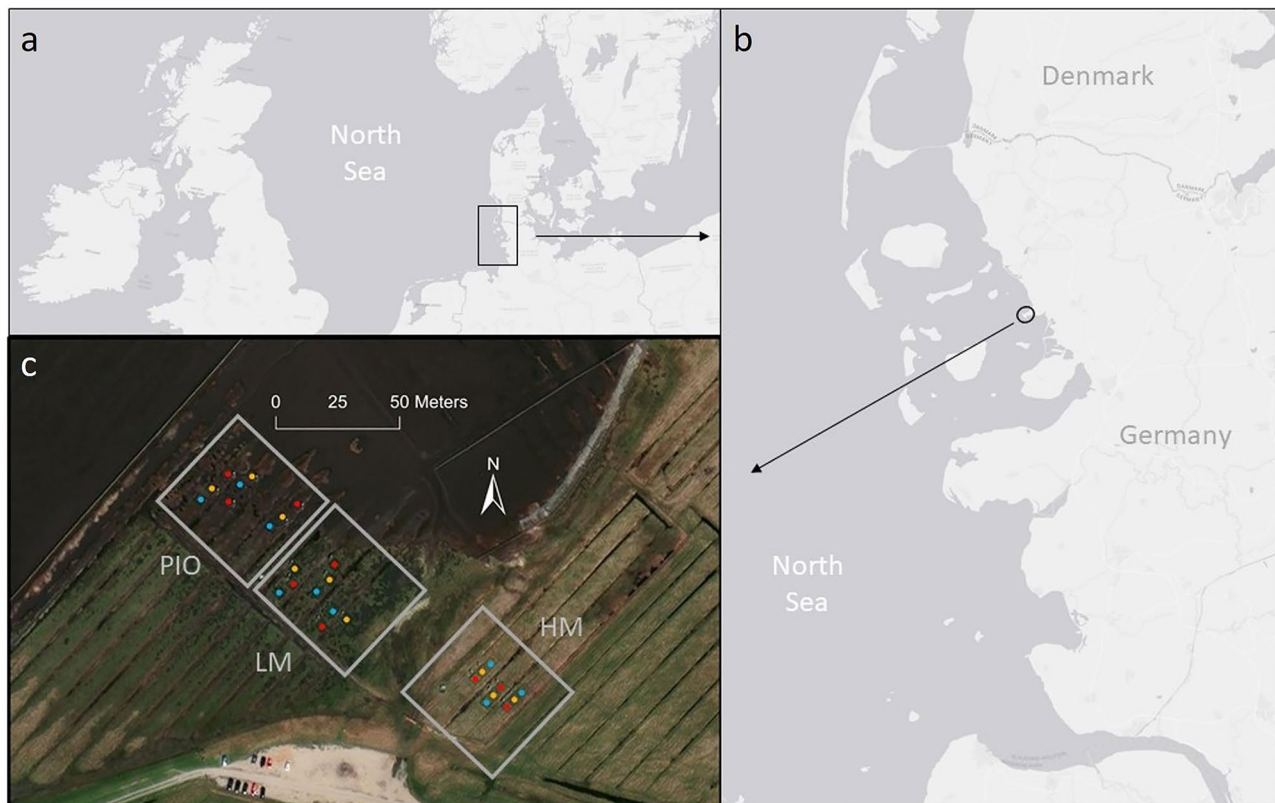


Figure 2. (a, b) Location of the Marsh Ecosystem Response to Increased Temperatures experiment on Hamburger Hallig at the North Sea coast in Germany. (c) Warming treatment plot map (blue: ambient, orange: +1.5°C, and red: +3.0°C) within each of the three marsh zones (PIO, pioneer; LM, low marsh; HM, high marsh).

fields (Palm, 2000). From 2018 to 2020, mean annual temperature was 10.2°C, mean annual precipitation was 1,047.6 mm, and mean annual wind speed was 5.41 m s⁻¹, with gusts exceeding 13.9 m s⁻¹. During the study period (yday 81–235 in 2019), mean daily temperature ranged from 13.2 to 14.9°C and mean daily windspeed ranged from 4.9 to 5.3 m/s (Reußenköge, meteo-stat.net). Mean tidal amplitude at the site is 3.4 m. Accretion ranges from 3.0 to 12.9 mm yr⁻¹ (Nolte et al., 2013b). The soils are gleysols (below mean high-tide waterline) and solonchaks (above mean high-tide waterline) according to the WRB soil classification system and predominantly consist of mineral silt (2–63 μm) (IUSS Working Group WRB, 2022; Nolte et al., 2013b). Soil organic matter contents are ~5% organic matter (Nolte et al., 2013b).

Three distinct marsh zones can be distinguished at the site (Figure 2c). The PIO is the lowest elevation zone and is flooded daily. PIO vegetation is dominated by *Spartina anglica* and *Salicornia europaea* with a mean canopy height of 23.9 cm. The LM is flooded less frequently, mainly during spring tides. Its vegetation is a diverse, heterogeneous mixture of species including *Puccinellia maritima*, *Atriplex portulacoides*, and *Limonium vulgare* with a mean canopy height of 21.9 cm. The HM has the highest elevation and is flooded only occasionally, mainly during storm tides in autumn and winter. Vegetation is dominated by *Elymus athericus* with a mean canopy height of 29.9 cm.

2.2. Experimental Design and Monitoring of Site Conditions

MERIT features three 8.0 m² replicate plots with three temperature levels (ambient, +1.5°C, and +3.0°C) in each of the three marsh zones (PIO, LM, HM) for a total of 27 plots (Figure 2c). The novel experimental approach—including its seasonal duration (March to October) and heating methods—is constrained by the extreme conditions of the high-energy coastal environment at the study site. Sensitive electrical components of the experiment are taken off-site in early October and are re-installed in late March.

To monitor dynamics of abiotic conditions at the study site, water level sensors and a meteorological (MET) station were deployed in spring 2019 at 3 m height to collect precipitation, wind speed and direction, air temperature,

and relative humidity (MaxiMet GMX600), as well as net solar radiation and photosynthetically active radiation (LI200R and LI190R, Licor Biosciences, USA). Flooding duration and frequency were assessed by two water level sensors (CS456, Campbell Scientific, USA), which were deployed below the soil surface in fabric-protected monitoring wells. One well was installed in the HM and the other between PIO and LM.

Surface elevation relative to the German Ordnance Datum (NHN) was established for all 27 experimental plots (LL500 laser and HR500, receiver Trimble, USA). Individual plot flooding events were established by reconciling water level records with surface elevations. As expected, tidal flooding frequency was highest in PIO and occurred almost daily, while LM flooded approximately two times a month during spring tides (Figure S1 in Supporting Information S1). Storm tides occasionally inundate the entire site and in 2019, the HM was occasionally flooded during the field season (Figure S1 in Supporting Information S1). Normalized Difference Vegetation Index was also monitored in each plot (model-SRS, Meter Group, USA).

2.3. Passive Aboveground Warming

Aboveground warming was applied by passive warming domes constructed to retain heat and trap incoming solar radiation (Figure 3a). These domes were assembled from 12 identical bent aluminum tubes (40 mm ID, schedule 40) and connected with cast aluminum Kee clamps (Kee Safety, Buffalo NY, USA). All frames are cable-anchored into the soil and remain in place during the growing season (early April to mid-October). The domes are covered with differing amounts of 32.43 cm wide transparent and UV- and saltwater-resistant PVC film for each temperature treatment (Gloflex CRISTAL MAR 500; 0.5 mm). The film is arranged in horizontal strips and attached to the aluminum frame using plastic greenhouse clips. Gaps (10–20 cm) between strips allow rainwater and tidal currents to enter the plots. Domes in the +1.5°C and +3.0°C warming treatments are covered with a total of 7.9 m² (38% of dome surface area) and 13.6 m² (65% of surface area) of PVC film, respectively. Ambient treatment plots are equipped with an aluminum frame without PVC film. Tests showed only minimal impacts of the film coverings on light availability or incoming precipitation (data not shown).

2.4. Active Surface and Belowground Warming

Soil warming is accomplished through a combination of horizontal surface heating cable systems (Bergh & Linder, 1999; Peterjohn et al., 1993) and deep soil heating techniques (Hanson et al., 2017; Rich et al., unpublished; Figures 3b and 3c). To our knowledge, only one other experiment combines these two types of soil heating elements (Pries et al., 2017). Warming pins were fabricated from resistance heating cables (GX 088L3100, 9.8 Ω/m, Danfoss, Denmark). The 31 pins per plot are 1 m long and 8 mm in diameter, spaced 64 cm equidistant from each other, and wired in parallel to operate on 12 V AC. This design has a minimal footprint, causing only minor disturbance when the pin is inserted and has very low maximum energy requirements (312 Wm⁻²). A secondary heating mechanism is a 52 m resistance heating cable (GX-088L3106 GX, 9.8 Ω/m, 240 V) sinuously deployed at the soil surface with 20 cm horizontal spacing (Figure 3b).

The overall horizontal footprint of vertical pins and surface heating cables was 3.2–3.84 m and extended beyond the passive dome footprint which was 3 × 3 m.

2.5. Monitoring and Control

Aboveground temperatures were monitored in all plots: air temperature was monitored at 75 cm above the soil surface by an epoxy-coated thermistor with minimal profile (air thermistor; T_{air}), and by a second thermistor embedded in an acrylic plate (101.6 × 101.6 × 6.35 mm) at ~30 cm in PIO and LM and at ~70 cm in HM (above thermistor; T_{above}). This second aboveground plate sensor is a standard way that canopy temperature is monitored in warming experiments where infrared radiation (IR) heating is used (Noyce et al., 2019; Reich et al., 2020; Rich et al., 2015). Sensor data was measured using an Arduino brand data logger (Code Supplement). All thermistors were fabricated by the MERIT team based on the Therm109 sensor specification (Campbell Scientific, USA) using identical resistance components. Temperature calculations were based on the Steinhart-Hart equation for the Therm109 sensor.

Belowground, a variety of thermistors based on the Therm109 design and embedded with marine epoxy into an 8.45Ø mm fiberglass-wound tube (Goodwinds, USA) were deployed in all plots. To control the heating rate for

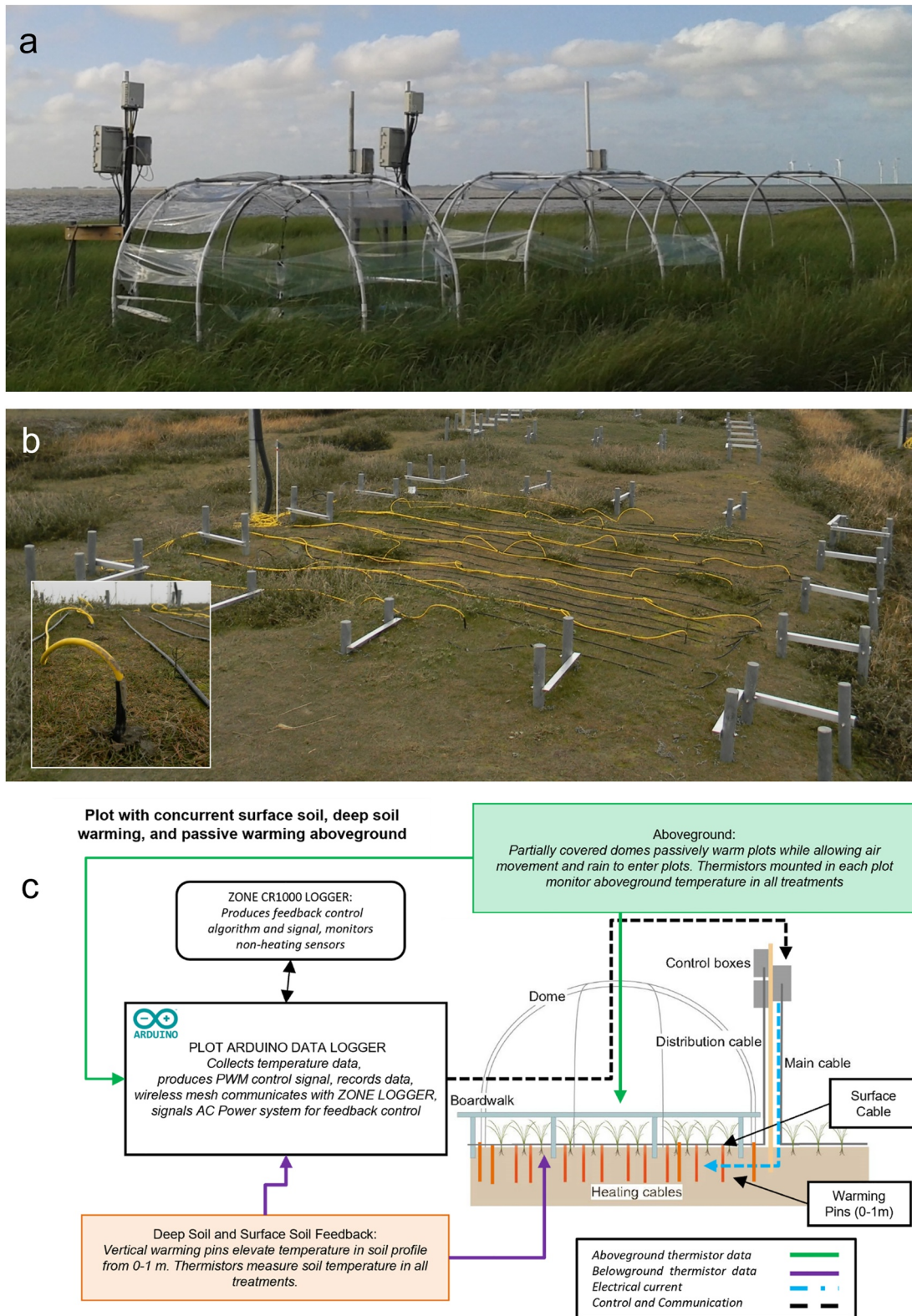


Figure 3. (a) Examples of three domes with different amounts of cover representing the ambient, +1.5°C, and +3.0°C temperature treatments; (b) Position of deep warming pins and surface warming cables in sample plot; and (c) Schematic of the feedback control system for experimental warming (side view, dome not to scale).

deep warming, a below thermistor (T_{below}) was installed at 25 cm depth and positioned <5 cm from warming pins. A lag thermistor (T_{lag}) also was installed at 25 cm depth but positioned 32 cm from heating pins to track warming farthest away from heating pins. A deep thermistor (T_{deep}) was placed at 75 cm depth and positioned ~5 cm from warming pins. A surface thermistor (T_{surface}) was positioned 3 cm away from horizontal cables at 5 cm depth.

The belowground warming system used microprocessor-based feedback control to maintain a fixed temperature difference (either +1.5°C or +3.0°C) between warmed and ambient control plots at the soil surface (calculated at 5 cm depth; T_{surface}) and in deeper soils (calculated at 25 cm depth; T_{below}) (Figure 3c). These systems independently operate the horizontal soil surface cable and the deep soil warming pins, respectively. Control was executed every 10 s at the marsh zone (PIO, LM, HM) scale by maintaining a targeted difference (+1.5°C or +3.0°C) between the average of ambient replicates in each zone (3 plots) and individual warmed plots in that zone. Heating calculations were completed by marsh zone-level CR1000 programs. Arduino dataloggers and Campbell CR1000 loggers share sensor and control data using modbus communication protocols via an Xbee (Digi, USA) wireless mesh network.

Control signals from Arduino dataloggers modulated zero crossing solid state relays (CWD2425 from Crydom) on a 4 s duty cycle to control surface cables or heating pins. Via this system, the power to each resistance heater pulses for a portion of the interval and thus controls power output to resistance heating equipment. The close proximity of the controlling temperature sensors (T_{below} or T_{surface}) to the heating elements tightly controls heating rate and minimizes overheating risks to the soil. Thermal diffusivity distributes warming through the plot (Noyce et al., 2019; Rich et al., 2015) (Figure 3). Generally, it took less than 24 hr for plots to reach target delta temperatures. Contingency programming allows sensor data from neighboring plots of the same warming treatment to substitute values when sensors were offline or out of range (Code Supplement). Power was supplied via connection to grid AC. We calculated estimated kilowatt-hour (kWh) usage for both heating systems using average hourly usage and wattage capacity—0.455 kWh at 12 V for deep heaters and 1.9 kWh at 230 V for surface heaters.

2.6. Data Processing

Thermistor data from the sensors at each plot (T_{surface} , T_{below} , T_{lag} , T_{deep} , T_{air} , and T_{above}) were polled every 3 min by the zone-scale feedback control program. The program flags suspect data based on a 15-min moving window standard deviation computation; data greater than ± 1.5 standard deviations away was considered suspect and removed from the control algorithm and flagged. Sensors that recorded errors were taken offline with respect to the feedback control data stream until they were replaced or repaired.

At the onset of the experiment, T_{above} plate sensors in PIO experienced failures, as they were not adequately waterproofed for daily tidal flooding. This resulted in a loss of data during the first half of the 2019 field season in the PIO zone. We have not included this parameter for PIO zone analyses. Our soil thermistors also had a high initial failure rate due to unexpected water intrusion and were replaced throughout 2019; we prioritized replacing T_{below} as opposed to T_{lag} sensors because T_{below} controls feedback heating of deep soil warming pins. These gaps in the T_{lag} data limit its use overall but still allow assessment of horizontal distribution of deep heating.

To assess the warming treatments and experimental design, we used thermistor data stored on Arduino loggers for each plot. Data was cleaned based on methods expanded from Rich et al. (2015). A range limitation function was applied to remove data points that deviated more than $\pm 5^\circ\text{C}$ (T_{surface} , T_{below} , T_{lag} , T_{deep}) and $\pm 10^\circ\text{C}$ (T_{air} , T_{above}) from the mean hourly observed data for all plots in the same marsh zone. To detect electronic noise and intermittent thermistor failures, we calculated standard deviation of temperature for 1-hr and 48-hr moving windows for each sensor. Any individual value that was outside the 0.95 quantile of each moving window was removed. The net effect of these filters was to remove data that may not have registered a value (dropped data) or to remove values that were indicative of electronic noise, such as voltage spikes. For example, reset events in our experimental control system created recognizable electronic noise. Additionally, each sensor data stream was visually assessed for issues like sensor location misplacement, which could be observed by sudden level shifts. Data from ambient sensors that were moved suddenly or were mispositioned were removed from data processing of warming treatment delta (ΔT) calculations. Given the high energy environment, amplitude of tides, and number of sensors at the MERIT field site, issues of these types were expected. Ultimately, we removed ~10% of sensor data based on these criteria, primarily from T_{lag} and T_{above} data.

Table 1
Means Comparison (ANOVA) of Ambient Air and Soil Temperatures by Marsh Zone

T _{air} °C				
	DF	SS	F Ratio	Prob > F
Zone	2	42.78902	0.6963	0.4984
	Mean	SE	L 95%	U 95%
HM	14.81	0.05	14.71	14.91
LM	14.89	0.05	14.80	14.99
PIO	14.85	0.05	14.75	14.94
T _{below} (−25 cm)				
	DF	SS	F Ratio	Prob > F
Zone	2	16285.28	641.9752	<0.0001
	Mean	SE	L 95%	U 95%
HM	13.23	0.03	13.17	13.29
LM	13.33	0.03	13.27	13.39
PIO	14.66	0.03	14.60	14.72
T _{surface} (−5 cm)				
	DF	SS	F Ratio	Prob > F
Zone	2	18163.9	547.5167	<0.0001
	Mean	SE	L 95%	U 95%
HM	13.59	0.04	13.52	13.66
LM	14.09	0.04	14.02	14.16
PIO	15.30	0.04	15.23	15.38
T _{deep} (−75 cm)				
	DF	SS	F Ratio	Prob > F
Zone	2	1171.019	55.394	<0.0001
	Mean	SE	L 95%	U 95%
HM	11.65	0.03	11.59	11.71
LM	12.03	0.03	11.98	12.09
PIO	12.05	0.04	11.98	12.12

Note. T_{surface} °C measured at the soil surface, T_{below} °C at 25 cm soil depth, and T_{deep} at 75 cm soil depth. Bold values indicate significant values.

2.7. Statistical Analysis

We used Linear Mixed Models with Residual Maximum Likelihood (REML; JMP Version 14, SAS Institute, Inc.) to evaluate the warming treatment effects versus other aspects of the experimental design, using temperature differences between warmed and ambient plots (ΔT_{air} , ΔT_{above} , $\Delta T_{\text{surface}}$, ΔT_{below} , ΔT_{deep}) as responses. Models included the fixed effects of marsh zone (PIO, LM, HM), wind speed (m s^{-1}), temperature treatment (ambient, +1.5°C, +3.0°C), mean solar radiation (W/m^2), and plot flooding (hours per day). Plot was included as a random effect (nested in marsh zone). We calculated ΔT_{air} , ΔT_{above} , $\Delta T_{\text{surface}}$, ΔT_{below} , ΔT_{lag} , and ΔT_{deep} from 15-min average data summarized to hourly values. Any subsequent data aggregations are based on hourly averages summarized to various time increments (as in Rich et al. (2015)). ANOVA was used to evaluate trends in ambient data across marsh zones. To assess warming treatment performance under differing wind regimes, hourly data was grouped into three classes of wind speed (<3.5, 3.5–7.0, and >7.0 m s^{-1}). Because of sensor issues, Figure 9 summary data presented for aboveground- and air temperature-derived parameters uses data initially summarized weekly by hour \times plot \times zone to represent the warming treatments throughout the field season, regardless of the number of overall observations. Statistics were calculated with R (<https://r-project.org/>) and REML mixed models were calculated in JMP14 (<https://jmp.com>).

3. Results

Under ambient conditions, mean air temperature did not differ between marsh zones (ANOVA $p > 0.05$, Table 1), whereas mean soil temperature was significantly affected by marsh zone (ANOVA $p < 0.0001$ for T_{surface}, T_{below}, and T_{deep}, Table 1). Mean soil surface temperature (T_{surface}) in PIO was 1.1°C higher than in LM and 1.6°C higher than in HM. The 25 cm (T_{below}) depth had similar differences, while the temperature difference was about 50% lower at 75 cm depth (T_{deep}).

MERIT elevated temperature both above- and belowground in all three zones (PIO, LM, HM). Warming treatments were more consistent (+1.5°C and +3.0°C) in the feedback-controlled surface and belowground portions than in the passively warmed aboveground portion of the experiment. REML Mixed Models show significant effects of warming treatments for ΔT_{air} , ΔT_{above} , $\Delta T_{\text{surface}}$, and ΔT_{below} (Table 2). Belowground and at the surface, warming treatments dominate temperature differences. External factors such as wind speed, flooding, and incoming solar radiation increase in significance at the soil surface ($\Delta T_{\text{surface}}$) and aboveground (ΔT_{air} and ΔT_{above}). The pattern of feedback-controlled surface warming and belowground warming differs from the aboveground passive warming pattern. We split the reporting of results accordingly.

3.1. Active Surface- and Belowground-Warming

Overall fit was good for soil heating REML mixed model responses: $\Delta T_{\text{surface}}$ ($R^2 = 0.89$) and ΔT_{below} ($R^2 = 0.95$). Additionally, plot-to-plot variation within each marsh zone was less than 18% of total variation, indicating that individual plots in each zone received similar warming treatments (Table 2, Table S1 in Supporting Information S1). For $\Delta T_{\text{surface}}$ and ΔT_{below} responses, warming was the strongest fixed effect followed by flooding duration per day in both models (Table 2). The $\Delta T_{\text{surface}}$ model added average daily solar radiation as a significant fixed effect (Table 2). For both the active surface and belowground warming, mean temperature (T_{surface} and T_{below}, Figure 4a) increased in warmed plots and mean delta ($\Delta T_{\text{surface}}$ and ΔT_{below} , Figure 4b) matched warming targets. At the soil surface, the highest variation in mean soil temperatures and mean delta across all marsh zones and

Table 2
Fixed Effects Summary of Linear Mixed Models With Residual Error Maximum-Likelihood Proportioning for ΔT_{air} , ΔT_{above} , $\Delta T_{\text{surface}}$, and ΔT_{below} Responses

Fixed effect	ΔT_{air}				ΔT_{above}				ΔT_{below}				$\Delta T_{\text{surface}}$			
	DF	DFDen	F ratio	Prob > F	DFDen	F ratio	Prob > F	DFDen	DFDen	F ratio	Prob > F	DFDen	DFDen	F ratio	Prob > F	DFDen
Treatment	2	21.53	11.97	0.0003	14.04	40.52	<0.0001	22.00	1,329.98	0.17	0.6821	21.98	8653.00	428.77	<0.0001	0.0026
Wind_speed_avg/day	1	8421.00	137.23	<0.0001	5703.00	393.57	<0.0001	8755.00	8763.00	12.23	0.0005	8660.00	113.72	58.25	<0.0001	0.992
Plot hrs/day flooded	1	8428.00	4.50	0.0339	5701.00	2.48	0.0471	8754.00	22.20	0.07	0.934	22.18	0.01	0.01	0.992	0.992
Solar radiation avg/day	1	8419.00	1369.18	<0.0001	5701.00	995.27	<0.0001	8754.00	22.20	0.07	0.934	22.18	0.01	0.01	0.992	0.992
Zone	2	21.76	2.15	0.1402	14.10	2.15	0.1376	22.20	0.07	0.934	0.934	22.18	0.01	0.01	0.992	0.992

Note. Models shown are daily scale aggregations with separations for day versus night. DFDen is the degrees of freedom used in denominator of each test (n-k-1). Additional summary data in Table S1 in Supporting Information S1. Bold values indicate significant values.

plots ranged from 1.43° to 1.67°C for the +1.5° treatment, and 2.54° to 2.99°C for the +3.0° treatment. Mean temperature variation was lower and warming treatment effects decreased at 75 cm below the soil surface (T_{deep} , Figures 4a and 4b). Here, delta values ranged from 1.14° to 1.43°C for the +1.5° treatment and 1.92° to 2.36°C for the +3.0° treatment. At 25 cm depth, we observed delta values ranging from 1.51° to 1.55°C for the +1.5° treatment and 2.87° to 3.02° for the +3.0° treatment (T_{below} , Figure 4b).

Soil warming at all depths was consistent throughout the duration of the experiment (Figure 5; Figures S2 and S3 in Supporting Information S1). Surface and belowground temperature distributions for +1.5° and +3.0°C treatments shifted in mean but matched ambient distributions (Figure 6). Diurnally, mean delta values diminished slightly at midday—when plots are warmest (Figure 7). Tidal flooding created minor reductions in soil warming treatments as compared to non-flooded intervals. In PIO, the highest reductions were observed at the soil surface, where mean warming treatment delta reductions were −0.23°C and −0.21°C in the +1.5° and +3.0° treatments, respectively (Figure 8).

3.2. Passive Aboveground Warming

Levels of passive aboveground warming were efficacious but lower than the precise feedback-controlled warming achieved belowground (Figures 9a and 9b). We observed only minor shifts in overall field season temperature distribution (Figure 9c) by aboveground warming. REML mixed model overall fit was less than belowground responses with $R^2 = 0.30$ for ΔT_{air} and $R^2 = 0.41$ for ΔT_{above} (Table 2, Table S1 in Supporting Information S1). Plot-to-plot variation within each marsh zone was low and similar to belowground responses (Table 2, Table S1 in Supporting Information S1). For ΔT_{air} and ΔT_{above} responses, the magnitude of fixed effects differed from belowground; average daily solar radiation was the largest significant fixed effect followed by average wind speed and then the warming dome treatment itself (Table 2). Warming was primarily achieved during daytime, with deltas greatly exceeding overall mean deltas (Figure S4 in Supporting Information S1). During the day, ΔT_{air} was 0.34°–0.60°C in the +1.5°C treatments and 0.55°–1.18°C in the +3.0°C treatments, with greater warming in HM, followed by PIO and LM (Figure S4 in Supporting Information S1). For ΔT_{above} , mean deltas were 0.65°–0.66°C in the +1.5°C treatments and 0.95°–1.11°C in the +3.0°C treatments, with greater warming in the LM than in the HM (Figure S4 in Supporting Information S1). Due to flooding-induced sensor unreliability, we have not included data from aboveground plate sensors (ΔT_{above}) in PIO (Figure S4 in Supporting Information S1). Delta values from aboveground plate sensors (ΔT_{above}) were greater at night than those of air sensors (ΔT_{air}) (Figure S4 in Supporting Information S1).

Mean ΔT_{air} decreased with increasing wind speed class during the day and at night (Figure 10a). Mean daily ΔT_{air} was correlated to incoming solar radiation ($R^2 = 0.20$ and 0.11, $F < 0.0001$ for +1.5 and +3.0 treatments; Figure 10b).

4. Discussion

The MERIT design is effective at warming a high-energy salt marsh at all three marsh zones (PIO, LM, HM) both above- and belowground. We discovered pronounced differences in ambient soil surface temperatures along the elevation gradient, with mean temperatures at PIO being 1.6°C higher than in HM. This agrees with Alber and O'Connell (2019) and is most likely an effect of lower vegetation cover and more open soil in PIO compared to HM. Overall, the performance of aboveground dome warming treatment was lower than belowground systems but matched or exceeded the performance of other passive OTC and IR warming systems under similar conditions (LeCain et al., 2015; Marion et al., 1997). Belowground heating components performed well in developing and maintaining warming treatments. The MERIT experimental approach thus provides a realistic and novel pathway to study salt marsh ecosystem responses to increased temperatures at high-energy coastal environments. For more information on Arduinos, dome performance, energy usage, sensor configuration, and design, see supplemental method and design notes. Below we assess warming performance at seasonal, daily, and diurnal timescales. A successful warming experiment would elevate temperature as compared to ambient at each of these scales.

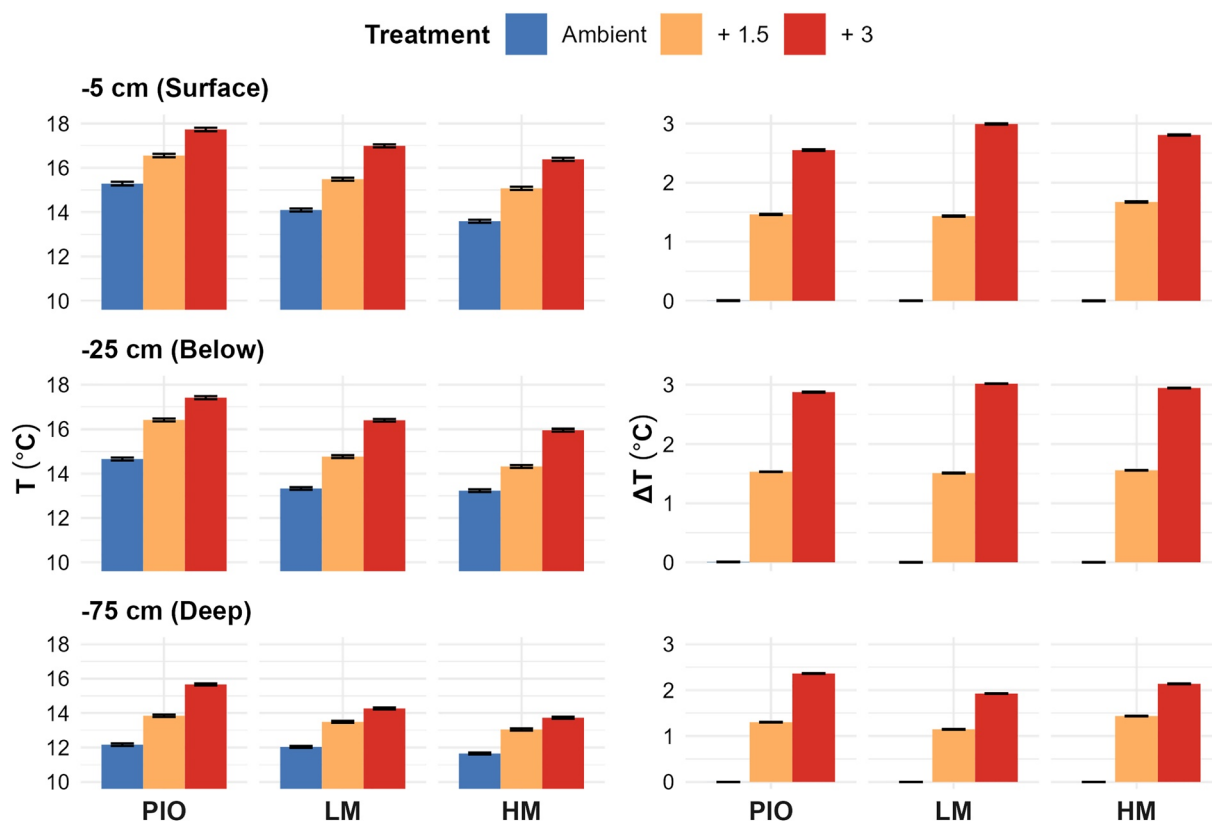


Figure 4. (a) Mean Temperature (T) and (b) Mean Delta (ΔT) of the 27 Marsh Ecosystem Response to Increased Temperatures plots measured in 2019 at 5 cm (T_{surface}), 25 cm (T_{below}), and 75 cm (T_{deep}) soil depths with 95% CI bars for marsh zones (PIO, pioneer; LM, low marsh; HM, high marsh) and temperature treatments (ambient (blue), +1.5°C (orange), and +3.0°C (red)).

4.1. Belowground and Soil Surface Warming

The feedback-controlled warming applied at MERIT effectively heats soils in a high-energy tidal wetland. This approach is a clear improvement over OTC-only experiments where minimal or diurnally unstable soil warming occurs (Carey et al., 2018). Feedback-controlled belowground warming systems have previously been used in a handful of experiments, mainly in terrestrial ecosystems (Peterjohn et al., 1993; Pries et al., 2017; Reich et al., 2020; Rich et al., 2015). We are aware of only two other experiments in wetlands (Hanson et al., 2017; Noyce et al., 2019) that are less hydrologically dynamic than the MERIT site. Despite the site's challenging conditions, the feedback-controlled heating resulted in elevated temperatures that tracked ambient patterns well for both the soil surface and deeper parts of the soils to at least 75 cm, which is comparable to Hanson et al. (2017) and Noyce et al. (2019). Heat was well-distributed horizontally across plots. ΔT_{lag} , representing maximum distance from vertical pins, showed only minor reductions in ΔT compared to ΔT_{below} , which represents areas closer to vertical pins (Figure S5 in Supporting Information S1).

At a seasonal scale, the distributions of all observed temperatures during the field season shifted to warmer temperatures, in line with warming treatment targets (Figure 6). Day-to-day warming patterns tracked ambient patterns in $\Delta T_{\text{surface}}$, ΔT_{below} , and ΔT_{deep} with consistent treatment differentiation as well as diurnal patterning closer to the surface (Figure 7). On an hourly basis, $\Delta T_{\text{surface}}$ showed modest warming treatment reduction during midday while ΔT_{below} and ΔT_{deep} were stable. $\Delta T_{\text{surface}}$ midday delta reductions are a reduction in temperature differences between warming treatments, not overall temperature. This decrease in warming treatment occurs because daily natural surface warming is faster than the heating cables can respond. The effect was greatest in PIO and was minimal in HM, likely because of the more open canopy and darker soils in PIO. A similar effect was also observed by Rich et al. (2015) with soil exposure before leaf-out in forests.

The main challenge of this experiment was to increase temperatures in different soil depths despite conditions such as high wind speeds and tidal flooding. Our mixed model showed that wind speed was not a significant

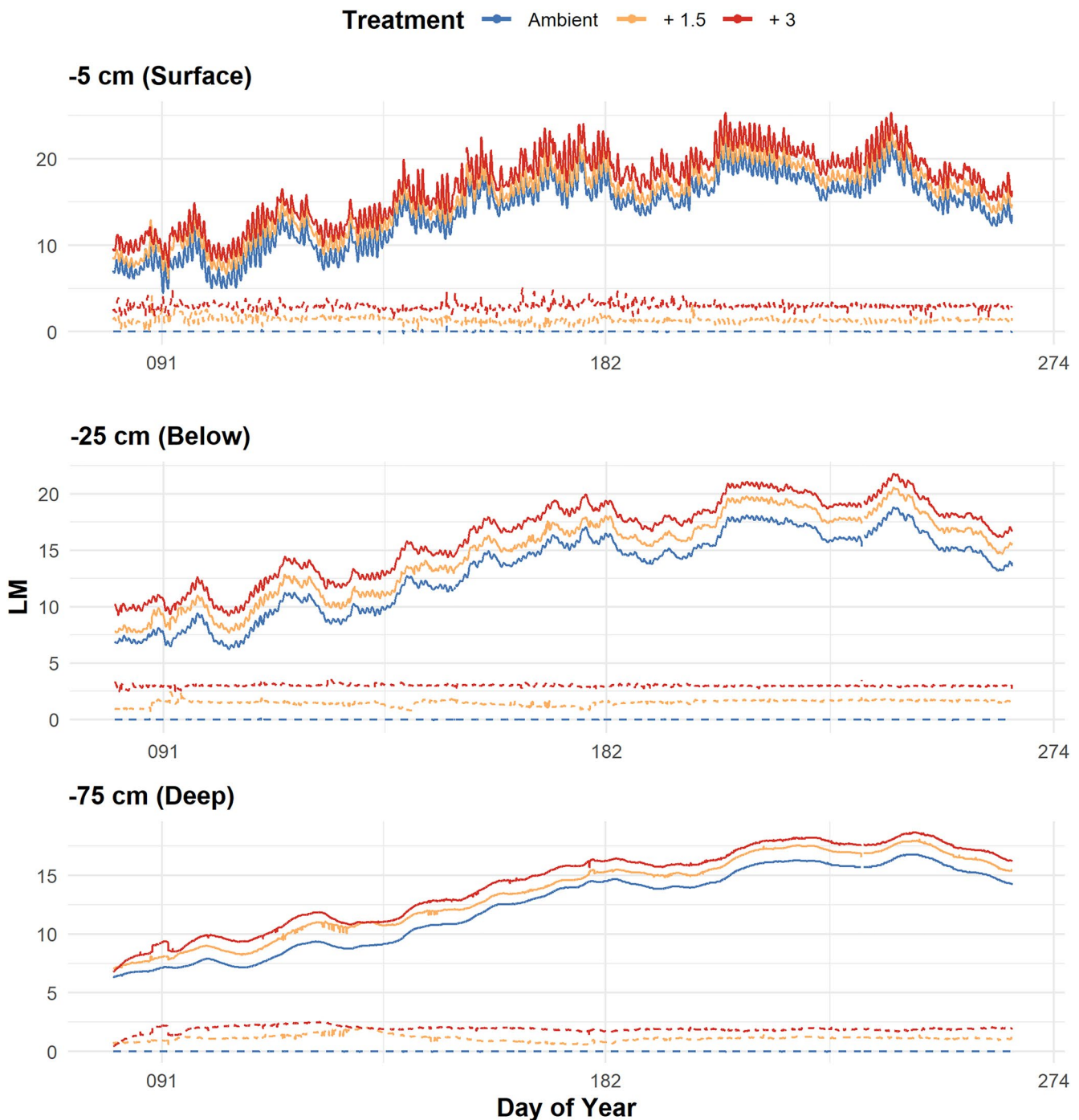


Figure 5. Mean Temperature (T, solid lines) and Mean Delta (ΔT , dotted lines) by hour and per warming treatments (ambient (blue), +1.5°C (orange), and +3.0°C (red)) for the nine Marsh Ecosystem Response to Increased Temperatures plots of the low marsh zone measured in 2019. Panels are differentiated for 5 cm (T_{surface}), 25 cm (T_{below}), and 75 cm (T_{deep}) soil depths.

factor for surface soil temperature or deeper soils. Modest reductions of $\Delta T_{\text{surface}}$ or ΔT_{below} during flooding were present (Figure 9) but did not occur in the deeper soil layers. Carey et al. (2018) and Zhong et al. (2013) report similar findings at the surface. Overall, the interactions of the surface feedback warming with hydrological and climatic factors were quite strong, and the differences in vegetation and albedo across the PIO, LM, and HM show how aboveground structural differences can influence the pattern and efficacy of warming treatments. We conclude that while other wetland warming experiments with low tidal flooding and dense vegetation do not need

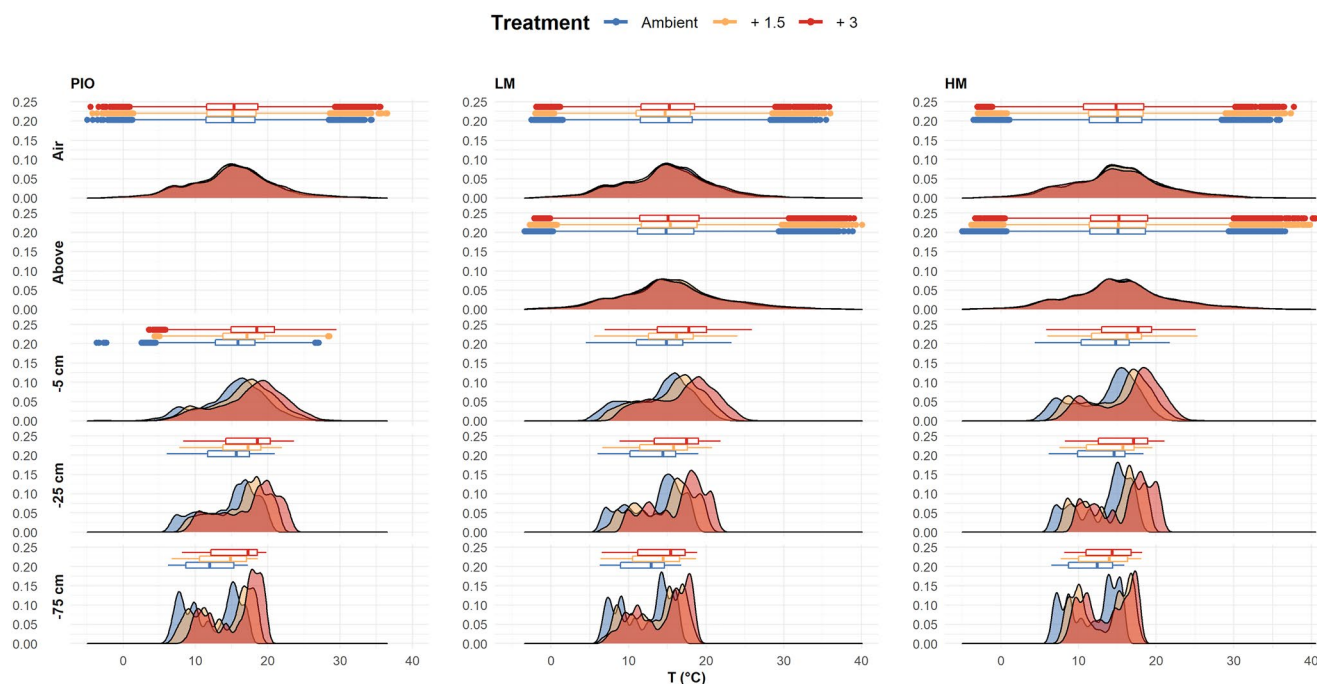


Figure 6. Density distributions of temperature values measured in the 27 Marsh Ecosystem Response to Increased Temperatures plots with three temperature treatments (ambient (blue), +1.5°C (orange), and +3.0°C (red)) in 2019. Panel density distributions are differentiated by zone (PIO, pioneer; LM, low marsh; HM, high marsh), and show sensors 30 cm above soil surface (T_{above}), 75 cm above soil surface (T_{air}), and at 5 cm (T_{surface}), 25 cm (T_{below}), and 75 cm (T_{deep}) soil depths.

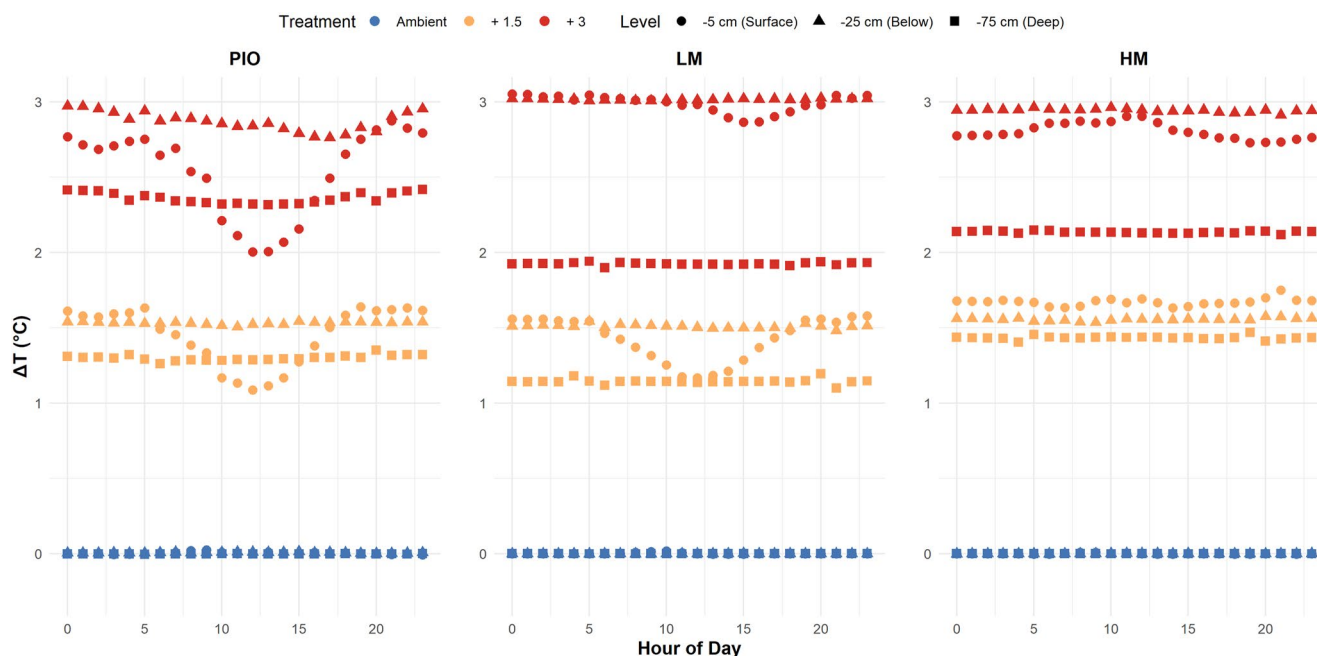


Figure 7. Mean temperature delta (ΔT) by hour of day per temperature treatment (ambient (blue), +1.5°C (orange), and +3.0°C (red)) and zone (PIO, pioneer; LM, low marsh; HM, high marsh) for soil sensors at 5 cm (T_{surface}), 25 cm (T_{below}), and 75 cm (T_{deep}) soil depths measured in the 27 Marsh Ecosystem Response to Increased Temperatures plots in 2019.

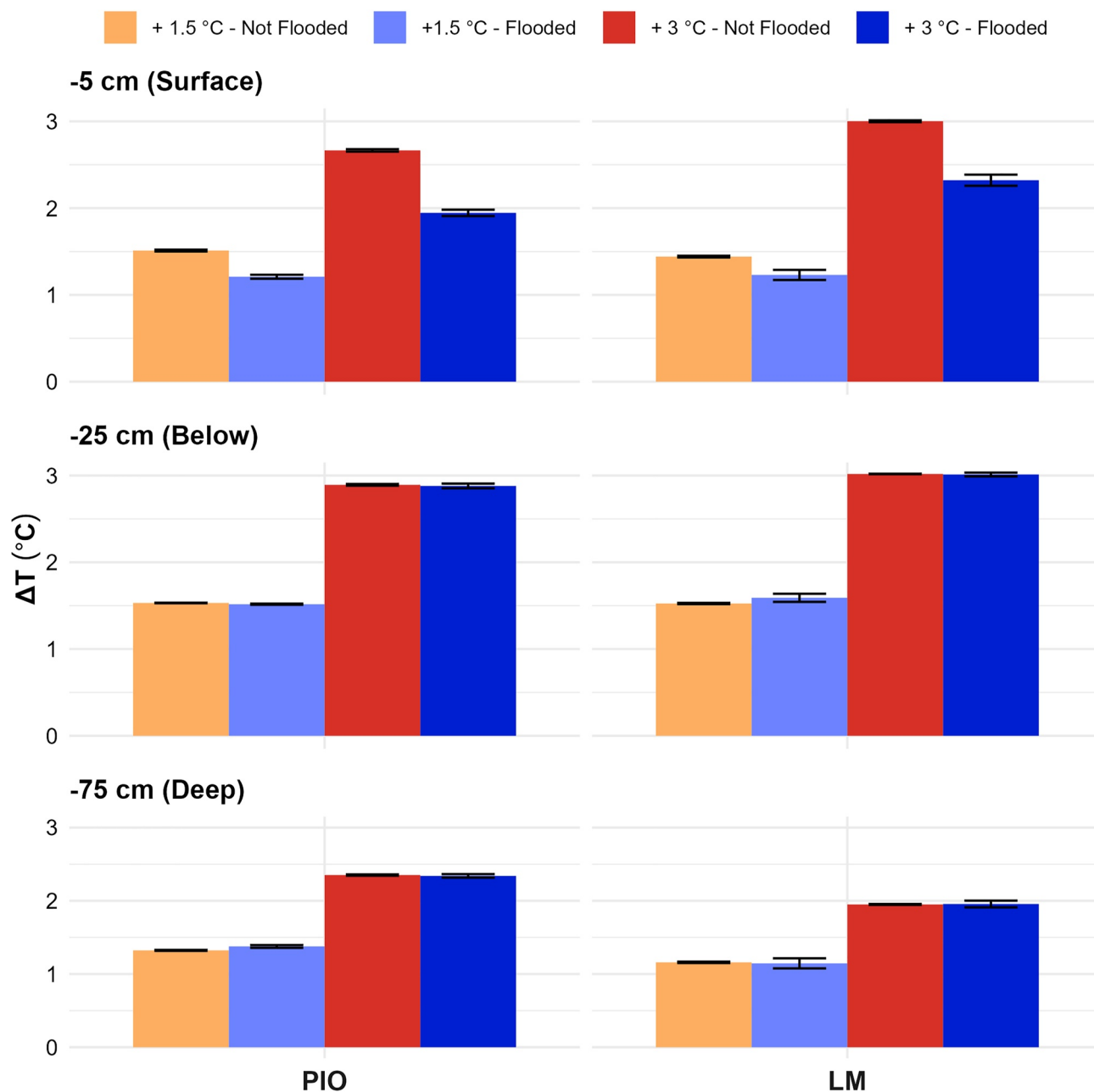


Figure 8. Mean soil temperature delta (ΔT) during flooded versus non-flooded periods at the soil surface (5 cm depth (T_{surface})) and at 25 cm (T_{below}) and 75 cm (T_{deep}) soil depths across warming treatments (+1.5 $^{\circ}\text{C}$ and +3.0 $^{\circ}\text{C}$) with 95% CI bars in the Marsh Ecosystem Response to Increased Temperatures experiment in 2019. As flooding occurred almost exclusively in the pioneer zone (PIO) and in the low marsh (LM), the graph is restricted to PIO and LM.

surface cable warming (Noyce et al., 2019), our results for MERIT suggest a need for surface cables to offset surface heat losses in this system.

4.2. Aboveground Warming

Aboveground warming treatments were significant and effective, but less so than belowground. Like other passive OTC experiments (Carey et al., 2018; Marion et al., 1997), larger daytime warming at our site was driven by increased incoming net solar radiation (Figures S5 in Supporting Information S1). ΔT_{air} increased with average hourly total radiation. Diurnally, we observed midday ΔT_{air} in the range of 0.9–2 $^{\circ}\text{C}$ (data not shown). Our peak average temperature occurred earlier in the day than observed in other experiments (Marion et al., 1997;

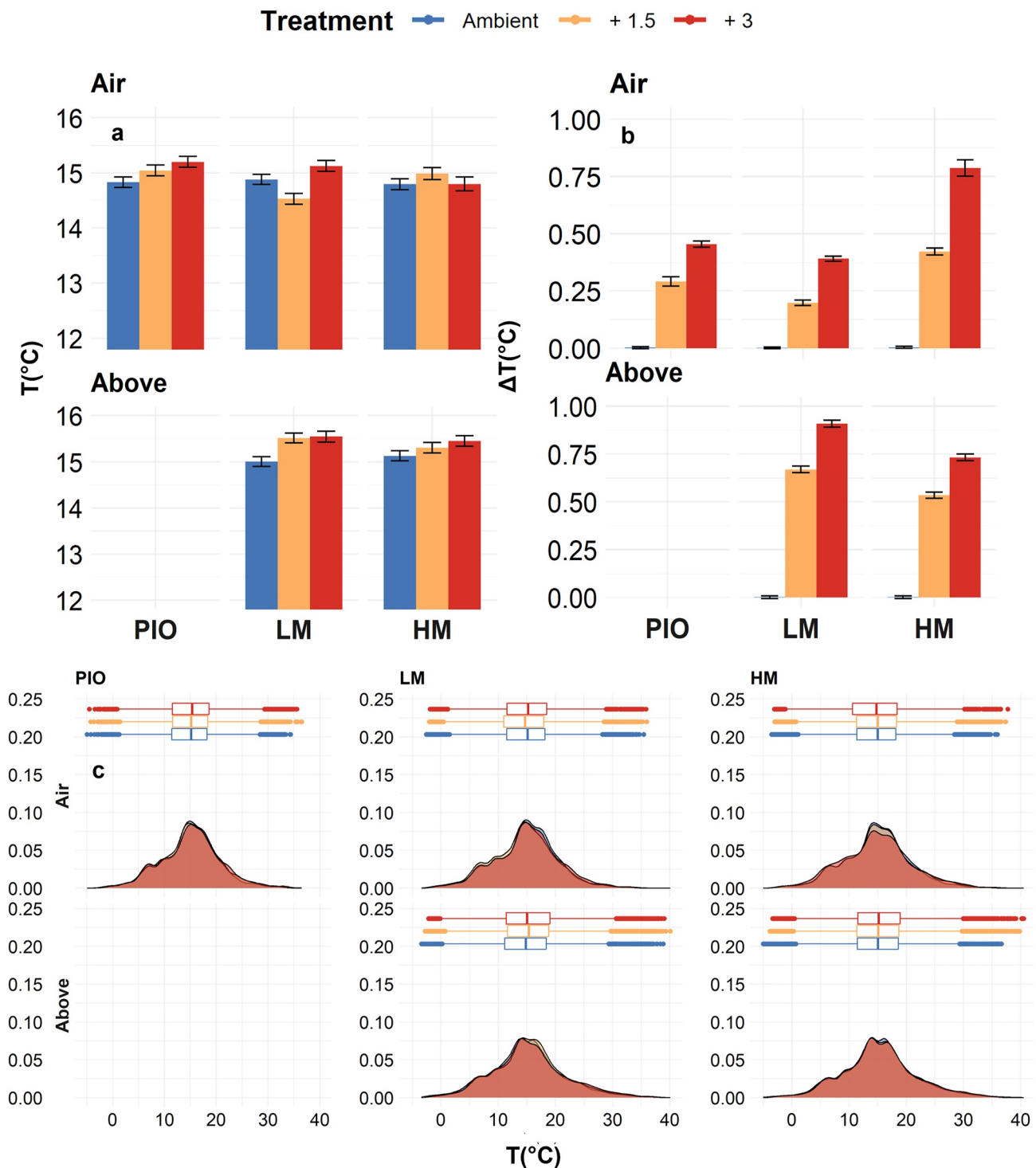


Figure 9. (a) Mean Temperature (T) and (b) Mean Delta (ΔT) of the 27 Marsh Ecosystem Response to Increased Temperatures (MERIT) plot temperatures measured in 2019 at T_{air} and T_{above} with 95% CI bars for marsh zones (PIO, pioneer; LM, low marsh; HM, high marsh) and temperature treatments (ambient (blue), +1.5°C (orange), and +3.0°C (red)). (c) Density distributions of temperature values measured in the 27 MERIT plots with three temperature treatments (ambient (blue), +1.5°C (orange), and +3.0°C (red)) in 2019. T_{air} and T_{above} density distributions are differentiated by zone (PIO, LM, and HM).

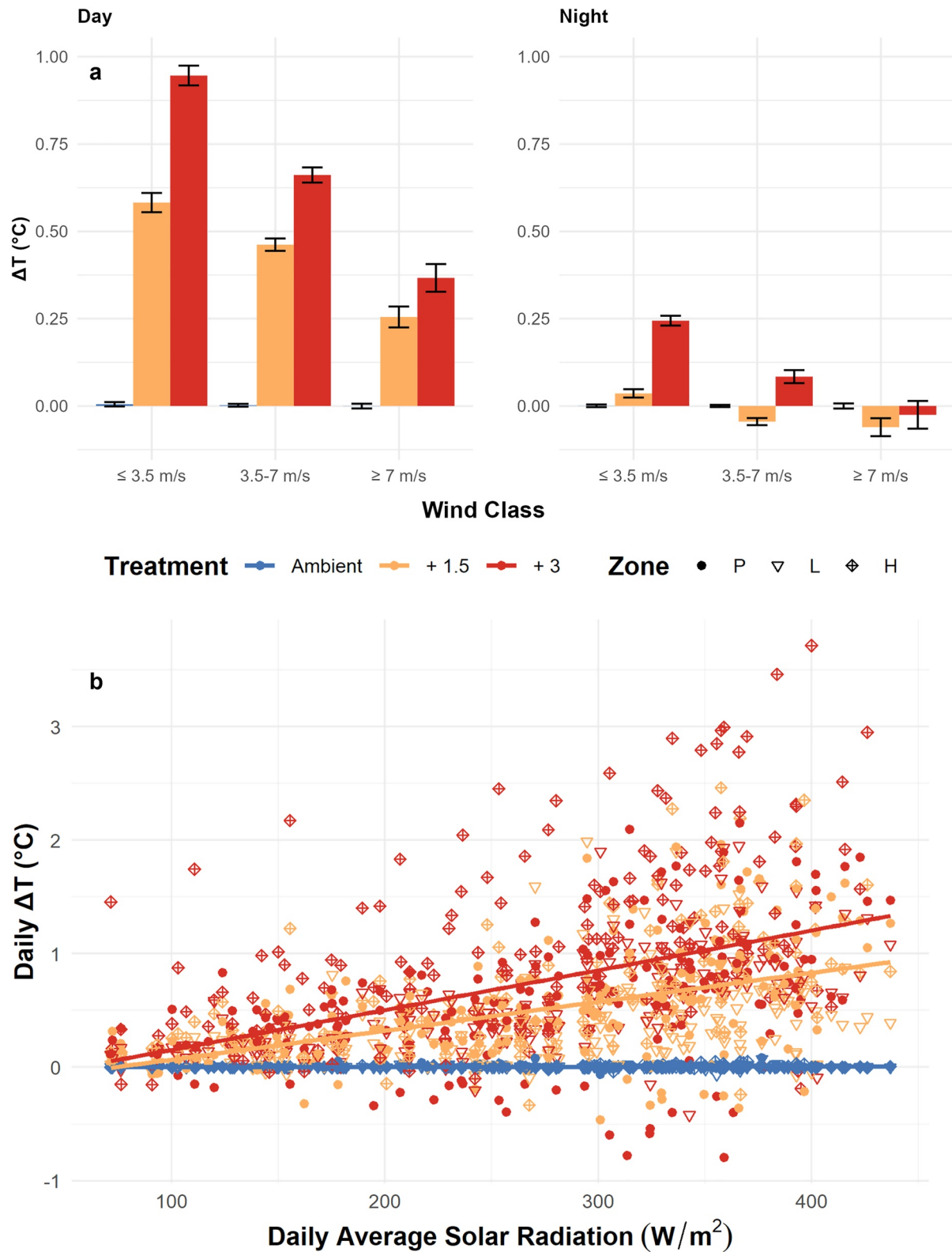


Figure 10. (a) Mean daytime air temperature delta (ΔT_{air}) by windspeed class (1: <3.5 m/s; 2: $3.5\text{--}7.0$ m/s, and 3: >7.0 m/s) during daytime and nighttime with 95% CI bars for the three temperature treatments (ambient (blue), $+1.5^{\circ}\text{C}$ (orange), and $+3.0^{\circ}\text{C}$ (red)). (b) Mean daytime air temperature delta per temperature treatment (ambient (blue), $+1.5^{\circ}\text{C}$ (orange), and $+3.0^{\circ}\text{C}$ (red)) and marsh zone (PIO, pioneer zone; LM, low marsh; HM, high marsh) versus daily average total radiation.

Rich et al., 2015); we attribute this to increasing afternoon wind speeds. We observed a modest but positive ΔT_{air} and ΔT_{above} at nighttime (Figure S4 in Supporting Information S1), which is different from other passive warming experiments where cooling at nighttime is often observed (Carey et al., 2018). Additionally, our data reveal that weeks with higher overall T_{air} also had higher ΔT_{air} . Our warming treatments were slightly greater in HM for ΔT_{air} compared to LM and PIO. The taller and denser plant canopy in HM might have reduced wind or air movement in the domes by covering the lowest gap between film pieces. ΔT_{air} was incrementally reduced with each wind speed level (<3.5, 3.5–7, and >7.0 m/s) (Figure 10a). ΔT_{air} became negligible at nighttime when wind speeds exceeded 7.0 m/s, accounting for approximately 2% of observations (Figure 10a).

Marion et al. (1997) compared several OTC designs in high wind speed conditions and found treatments were reduced to less than 1°C for wind speeds greater than 4 m s⁻¹. IR warming was considered; however, achievable active infrared warming in similarly windy sites was limited to just ~1°C (LeCain et al., 2015), and other IR warming experiments in sites with lower average wind speed reduce power when winds reach conditions comparable to MERIT (Rich et al., 2015). The performance of the MERIT aboveground warming treatments is as effective as IR warming and other OTC's given the site's overall wind speeds. The efficacy is constrained by external factors such as total incoming radiation and wind.

5. Conclusions

MERIT provides an effective method for warming salt marshes in high-energy coastal environments. Passive aboveground warming using film-covered domes in combination with feedback-controlled active surface and belowground heating provide a setup for understanding warming effects on this ecosystem while also capturing natural effects of strong winds, radiation, and tidal inundations. We expect that this experiment will open a pathway to understanding how warming may change the complex interactions between hydrology, vegetation, soil fauna, biogeochemistry, and sedimentation in salt marshes.

Global Research Collaboration

The primary location of this work is in Germany with some work in the United States. We have acknowledged local contributions to this work as needed and identified roles of authors in both the submission portal and in the authorship statement.

Data Availability Statement

All logger code and Arduino code will be publicly available through Github at corresponding author's Smithsonian Portal https://github.com/Smithsonian/MERIT_datalogger_code.

References

- Alber, M., & O'Connell, J. L. (2019). Elevation drives gradient in surface soil temperature within salt marshes. *Geophysical Research Letters*, 46(10), 5313–5322. <https://doi.org/10.1029/2019gl082374>
- Bergh, J., & Linder, S. E. (1999). Effects of soil warming during spring on photosynthetic recovery in boreal Norway spruce stands. *Global Change Biology*, 5(3), 245–253. <https://doi.org/10.1046/j.1365-2486.1999.00205.x>
- Carey, J. C., Kroeger, K. D., Zafari, B., & Tang, J. (2018). Passive experimental warming decouples air and sediment temperatures in a salt marsh. *Limnology and Oceanography: Methods*, 16(10), 640–648. <https://doi.org/10.1002/lom3.10270>
- Charles, H., & Dukes, J. S. (2009). Effects of warming and altered precipitation on plant and nutrient dynamics of a New England salt marsh. *Ecological Applications*, 19(7), 1758–1773. <https://doi.org/10.1890/08-0172.1>
- Duarte, C. M., Losada, I. J., Hendriks, I. E., Mazarrasa, I., & Marbà, N. (2013). The role of coastal plant communities for climate change mitigation and adaptation. *Nature Climate Change*, 3(11), 961–968. <https://doi.org/10.1038/nclimate1970>
- Fagherazzi, S., Kirwan, M. L., Mudd, S. M., Guntenspergen, G. R., Temmerman, S., D'Alpaos, A., et al. (2012). Numerical models of salt marsh evolution: Ecological, geomorphic, and climatic factors. *Reviews of Geophysics*, 50, 1–28. <https://doi.org/10.1029/2011rg000359>
- Gedan, K. B., & Bertness, M. D. (2010). How will warming affect the salt marsh foundation species *Spartina patens* and its ecological role? *Oecologia*, 164(2), 479–487. <https://doi.org/10.1007/s00442-010-1661-x>
- Hanson, P. J., Riggs, J. S., Nettles, W. R., Phillips, J. R., Krassovski, M. B., Hook, L. A., et al. (2017). Attaining whole-ecosystem warming using air and deep-soil heating methods with an elevated CO₂ atmosphere. *Biogeosciences*, 14(4), 861–883. <https://doi.org/10.5194/bg-14-861-2017>
- Hopple, A. M., Wilson, R. M., Kolton, M., Zalman, C. A., Chanton, J. P., Kostka, J., et al. (2020). Massive peatland carbon banks vulnerable to rising temperatures. *Nature Communications*, 11, 1. <https://doi.org/10.1038/s41467-020-16311-8>
- IUSS Working Group WRB. (2022). *World Reference Base for Soil Resources. International soil classification system for naming soils and creating legends for soil maps* (4th ed.). International Union of Soil Sciences (IUSS).

Acknowledgments

We thank Dr. Martin Stock, Armin Jess, and the Schleswig-Holstein Wadden Sea National Park for support in establishing MERIT at their site. The initial set-up of the warming experiment was paid through a Grant of Universität Hamburg to Kai Jensen. Roy Rich and Allegra Tashjian were supported through Contract 4500383502 between Smithsonian and Universität Hamburg, Smithsonian-MarineGEO, and the U.S. Department of Energy, BER DE-SC0014413, DE-SC0019110. Peter Mueller was partly supported by the DAAD PRIME fellowship program, funded through BMBF, and by the German Research Foundation (DFG) Project 407270017. Eva Ostertag, Salomé Gonçalves-Huq, and Miriam Fuß were supported from Bauer-Hollmann Stiftung in the framework of the project WEPSS. Svenja Reents was funded by the German Research Foundation (DFG) Project 401564364. Hao Tang was supported from the China Scholarship Council. We are grateful to Claudia Mählmann for administrative support and thank Detlef Böhm and other colleagues from the Applied Plant Ecology group for assistance in MERIT's construction. We thank Tom Kamin, Jörn Ehlers, and Stefan Knaak for ongoing help and technical expertise. We thank Susanne Wohlfahrt for assistance in preparing Figure 1, as well as Selina Cheng and Rae Tennent for finalizing figures for publication. Open Access funding enabled and organized by Projekt DEAL.

- Kirwan, M. L., & Guntenspergen, G. R. (2012). Feedbacks between inundation, root production, and shoot growth in a rapidly submerging brackish marsh. *Journal of Ecology*, 100(3), 764–770. <https://doi.org/10.1111/j.1365-2745.2012.01957.x>
- Kirwan, M. L., & Guntenspergen, G. R. (2015). Response of plant productivity to experimental flooding in a stable and a submerging marsh. *Ecosystems*, 18(5), 903–913. <https://doi.org/10.1007/s10021-015-9870-0>
- Lecain, D., Smith, D., Morgan, J., Kimball, B. A., Pendall, E., & Miglietta, F. (2015). Microclimatic performance of a free-air warming and CO₂ enrichment experiment in windy Wyoming, USA. *PLoS One*, 10(2), e0116834. <https://doi.org/10.1371/journal.pone.0116834>
- Marion, G., Henry, G., Freckman, D., Johnstone, J., Jones, G., Jones, M., et al. (1997). Open-top designs for manipulating field temperature in high-latitude ecosystems. In *Global change biology* (Vol. 3, No. (1), pp. 20–32). Blackwell Science Ltd. <https://doi.org/10.1111/j.1365-2486.1997.gcb136.x>
- McLeod, E., Chmura, G. L., Bouillon, S., Salm, R., Björk, M., Duarte, C. M., et al. (2011). A blueprint for blue carbon: Toward an improved understanding of the role of vegetated coastal habitats in sequestering CO₂. *Frontiers in Ecology and the Environment*, 9(10), 552–560. <https://doi.org/10.1890/110004>
- Mcowen, C. J., Weatherdon, L. V., Van Bochove, J., Sullivan, E., Blyth, S., Zockler, C., et al. (2017). A global map of saltmarshes. *Biodiversity Data Journal*, 5, e11764. <https://doi.org/10.3897/bdj.5.e11764>
- Mueller, P., Granse, D., Nolte, S., Weingartner, M., Hoth, S., & Jensen, K. (2020). Unrecognized controls on microbial functioning in Blue Carbon ecosystems: The role of mineral enzyme stabilization and allochthonous substrate supply. *Ecology and Evolution*, 10(2), 998–1011. <https://doi.org/10.1002/ece3.5962>
- Mueller, P., Jensen, K., & Megonigal, J. P. (2016). Plants mediate soil organic matter decomposition in response to sea level rise. *Global Change Biology*, 22(1), 404–414. <https://doi.org/10.1111/gcb.13082>
- Nolte, S., Koppenaal, E. C., Esselink, P., Dijkema, K. S., Schuerch, M., De Groot, A. V., et al. (2013a). Measuring sedimentation in tidal marshes: A review on methods and their applicability in biogeomorphological studies. *Journal of Coastal Conservation*, 17(3), 301–325. <https://doi.org/10.1007/s11852-013-0238-3>
- Nolte, S., Müller, F., Schuerch, M., Wanner, A., Esselink, P., Bakker, J., & Jensen, K. (2013b). Does livestock grazing affect sediment deposition and accretion rates in salt marshes? *Estuarine, Coastal and Shelf Science*, 135, 296–305. <https://doi.org/10.1016/j.ecss.2013.10.026>
- Nolte, S., Wanner, A., Stock, M., & Jensen, K. (2019). *Elymus athericus* encroachment in Wadden Sea salt marshes is driven by surface elevation change. *Applied Vegetation Science*, 22(3), 454–464. <https://doi.org/10.1111/avsc.12443>
- Noyce, G. L., Kirwan, M. L., Rich, R. L., & Megonigal, J. P. (2019). Asynchronous nitrogen supply and demand produce nonlinear plant allocation responses to warming and elevated CO₂. *Proceedings of the National Academy of Sciences of the United States of America*, 116(43), 21623–21628. <https://doi.org/10.1073/pnas.1904990116>
- Palm, M. (2000). Die Entstehungsgeschichte des Vorlandes der Hamburger Hallig - Eine 616 kartographische Aufarbeitung. In M. Stock & K. Kiehl (Eds.), *Die Salzwiesen der 617 Hamburger Hallig*. Boyens Medien GmbH and Co. KG. (Schriftenreihe / Nationalpark 618 Schleswig-Holsteinisches Wattenmeer, 11).
- Pendleton, L., Donato, D. C., Murray, B. C., Crooks, S., Jenkins, W. A., Sifleet, S., et al. (2012). Estimating global “blue carbon” emissions from conversion and degradation of vegetated coastal ecosystems. *PLoS One*, 7(9), e43542. <https://doi.org/10.1371/journal.pone.0043542>
- Peterjohn, W. T., Melillo, J. M., Bowles, F. P., & Steudler, P. A. (1993). Soil warming and trace gas fluxes: Experimental design and preliminary flux results. *Oecologia*, 93(1), 18–24. <https://doi.org/10.1007/bf00321185>
- Pries, C. E. H., Castanha, C., Porras, R. C., & Torn, M. S. (2017). The whole-soil carbon flux in response to warming. *Science*, 355(6332), 1420–1423. <https://doi.org/10.1126/science.aal1319>
- Reents, S., Mueller, P., Tang, H., Jensen, K., & Nolte, S. (2021). Plant genotype determines biomass response to flooding frequency in tidal wetlands. *Biogeosciences*, 18(2), 403–411. <https://doi.org/10.5194/bg-18-403-2021>
- Reich, P. B., Hobbie, S. E., Lee, T. D., Rich, R., Pastore, M. A., & Worm, K. (2020). Synergistic effects of four climate change drivers on terrestrial carbon cycling. *Nature Geoscience*, 13(12), 787–793. <https://doi.org/10.1038/s41561-020-00657-1>
- Rich, R. L., Stefanski, A., Montgomery, R. A., Hobbie, S. E., Kimball, B. A., & Reich, P. B. (2015). Design and performance of combined infrared canopy and belowground warming in the B4WarmED (Boreal Forest Warming at an Ecotone in Danger) experiment. *Global Change Biology*, 21(6), 2334–2348. <https://doi.org/10.1111/gcb.12855>
- Temmerman, S., Meire, P., Bouma, T. J., Herman, M. J., Ysebaert, T., & De Vriend, H. J. (2013). Ecosystem-based coastal defense in the face of global change. *Nature*, 504(7478), 79–83. <https://doi.org/10.1038/nature12859>
- Wilson, R., Hopple, A., Tfaily, M., Sebestyen, S. D., Schadt, C. W., Pfeifer-Meister, L., et al. (2016). Stability of peatland carbon to rising temperatures. *Nature Communications*, 7, 1. <https://doi.org/10.1038/ncomms13723>
- Zhong, Q., Du, Q., Gong, J., Zhang, C., & Wang, K. (2013). Effects of in situ experimental air warming on the soil respiration in a coastal salt marsh reclaimed for agriculture. *Plant and Soil*, 371(1–2), 487–502. <https://doi.org/10.1007/s11104-013-1707-z>